IRAQI BULLETIN OF GEOLOGY AND MINING (IBGM)\
IRAQ GEOLOGICAL SURVEY (GEOSURV-IRAQ)

*IBGM (**2025**, Vol 21; Issue 1)* *39-56*

GROUNDWATER POTENTIAL MAPPING USING GEOSPATIAL APPROACHES COMBINED WITH ELECTRICAL RESISTIVITY TOMOGRAPHY IN BAZIAN BASIN, SULAYMANIYAH GOVERNORATE, IRAQI KURDISTAN REGION

Hawber Ata Karim[1*], Zana Rughzai[1], Azad Sangawi[1], and Bakhtiar Qader Aziz[1]

[1] Department of Earth Sciences and Petroleum, College of Science, University of Sulaimani, Sulaimani, Iraq.
***** *Corresponding author e-mail: hawber.karim@univsul.edu.iq*

Type of the Paper (Article)
Received: 02/ 08/ 2024
Accepted: 10/ 11/ 2024
Available online: 27/ 06/ 2025

Abstract

In the Bazian basin in northern Iraq, groundwater plays a crucial role in agriculture and other activities. Unfortunately, excessive legal and illegal well extraction over the past three decades has led to a significant decline in the water table. To address this challenge, the study combined geographic information system (GIS) data with Electrical Resistivity Tomography (ERT). The objective is to create a geospatial model for groundwater potential zoning using multi-criteria analysis techniques, supported by geophysical approaches. This study used seven thematic layers, including geology, rainfall, slope, lineament density, drainage density, land use/land cover, and runoff, and finally combined them with remote sensing data, Google Earth Engine, and conventional information within the GIS environment. Thematic layers were ranked based on their importance for groundwater potential and weighted using the multi-criteria decision analysis and Analytical Hierarchy Process (MCDA-AHP). Two-dimensional (2D) electrical resistivity tomography was conducted using the SYSCAL R1 PLUS along three profile lines distributed over the study area. The data were recorded using the Wenner – Schlumberger array, and the raw data were subsequently processed using the Res2dinv software. The resulting groundwater potential zones for the total area (362) km^2 (GWPZs) were categorized into five zones: very low, low, moderate, high, and very high. The covered area for each level was 4.4%, 8.9%, 34.3%, 32.7%, and 19.7%, respectively. Electrical resistivity tomography (ERT) and well extraction rates are used to validate groundwater potential zones (GWPZs). The results from three ERT profiles align with the potential zone map. Additionally, a second validation using extraction rates from 40 wells was used to confirm these findings.

Keywords: Electrical resistivity tomography; Analytical Hierarchy Process; Geographic Information System; GWPZs; GEE; Bazian Basin.

ISSN 1811-4539, EISSN 3005-3714
https://doi.org/10.59150/ibgm2101a03
IBGM: http://ibgm-iq.org/
Academic Scientific Journals: www.iasj.net

1. Introduction

Groundwater is a critical element of the hydrological cycle and exists beneath the earth's surface in the fissures and pore spaces in the soil, particles, and rock layers (Al-Garni, 2009; Das & Pal, 2019; Fitts, 2002; Kumari et al., 2021). The availability of this resource is essential for household, economic growth, and agricultural activities (Ayazi et al., 2010). The water demand has risen dramatically in the past few years, particularly in arid and semi-arid areas across the globe. In such areas, the ever-increasing need for water to support population necessities and advancements has exerted considerable pressure on the groundwater resource (Kumari et al., 2021). So, in this situation, the exploration and sustainability of groundwater resources become fundamental concepts, especially in the Bazian basin (BSB), due to the lack of permanent fresh surface water.

An enormous number of approaches have been applied by researchers to demarcate groundwater potential zones in the last few years. The most often employed techniques in this discipline include the AHP (Sangawi et al., 2023), frequency ratio (Al-Abadi et al., 2016; Rahmati et al., 2015), and weights of evidence (Madani & Niyazi, 2015). Logistic regression model methods (Ozdemir, 2011), decision tree model (Chenini et al., 2010); Linear Discriminant Analysis and artificial neural network (Naghibi et al., 2018), evidential belief function (Nampak et al., 2014), and random forest model (Naghibi et al., 2016).

Over the past few years, researchers have developed an approach for delineating the potential areas of groundwater resources using the analytical hierarchy process, which is the most adaptable, cost-effective, and easily understood tool of multi-criteria decision analysis (MCDA) techniques (Chowdhury et al., 2010; Hajkowicz & Higgins, 2008; Kaliraj et al., 2014; Sangawi et al., 2023). In their study, Chenini et al. (2010) found that the groundwater recharge zone can be efficiently mapped utilizing the MCDA approach in conjunction with GIS. In 1980, Thomas Saaty designed the Analytic Hierarchy Process (AHP) as a useful technique for handling difficult decision-making in groundwater-associated domains. It simplifies complicated decisions into pair-wise comparisons and synthesis (Arulbalaji et al., 2019). Moreover, many researchers have confirmed that combining Geographic Information System GIS, remote sensing RS, and AHP approaches to detect groundwater potential areas is both reliable and cost-effective (Andualem & Demeke, 2019; Jha et al., 2007; Karim & Al-Manmi, 2019; Singh et al., 2019). Although knowledge and literature reviews are crucial components of AHP, they may contribute to its ambiguity due to the subjective nature of expert judgments and the potential for conflicting information (Chowdary et al., 2013).

Some studies have revealed that geophysical surveys, such as Electrical Resistivity Tomography (ERT), combined with GIS and RS, are the most reliable and common tools for groundwater exploration. It can serve as an alternative method for validating and assessing groundwater potential zones (Al-Manmi & Rauf, 2016; Islami et al., 2018; Oh et al., 2011; Sonkamble et al., 2014; Venkateswaran et al., 2014). The fundamental principles of this approach mainly depend on the electrical resistivity, saturation of water, and pore volume of the geological rock units (Kowalsky et al., 2011).

Ahmed and Al-Manmi (2019) generated a groundwater potential map of a part of the Bazian basin using only the AHP technique. So, in order to accurately evaluate the presence of groundwater and subsurface geology in the area of interest, a combination of GIS, RS, well data, and ERT approaches is required. The primary goal of this investigation is to detect potential groundwater zones in the Bazian basin using a combination of GIS, RS, and AHP, and then verify the validity of the results using 2D ERT sections and available water wells. Finally, the novelty of this study comes from the implementation of two-step validations (ERT and available wells), which can be ultimately used as a scientific framework for more

2. Study Area Description

The Bazian basin, situated within the Sulaymaniyah governorate in the Iraqi Kurdistan region, encompasses an area of 362 Km^2. Geographically, this area extends from 35°27'00" to 35°45'00" N latitude and 45°58'00" E to 45°19'00" E longitude, as displayed in Figure 1. The elevation varies from 678 to 1421 m above sea level. The area is classified as a semi-arid region (Ahmed & Al-Manmi, 2019; Barzinji, 2003; Hamamin, 2011).

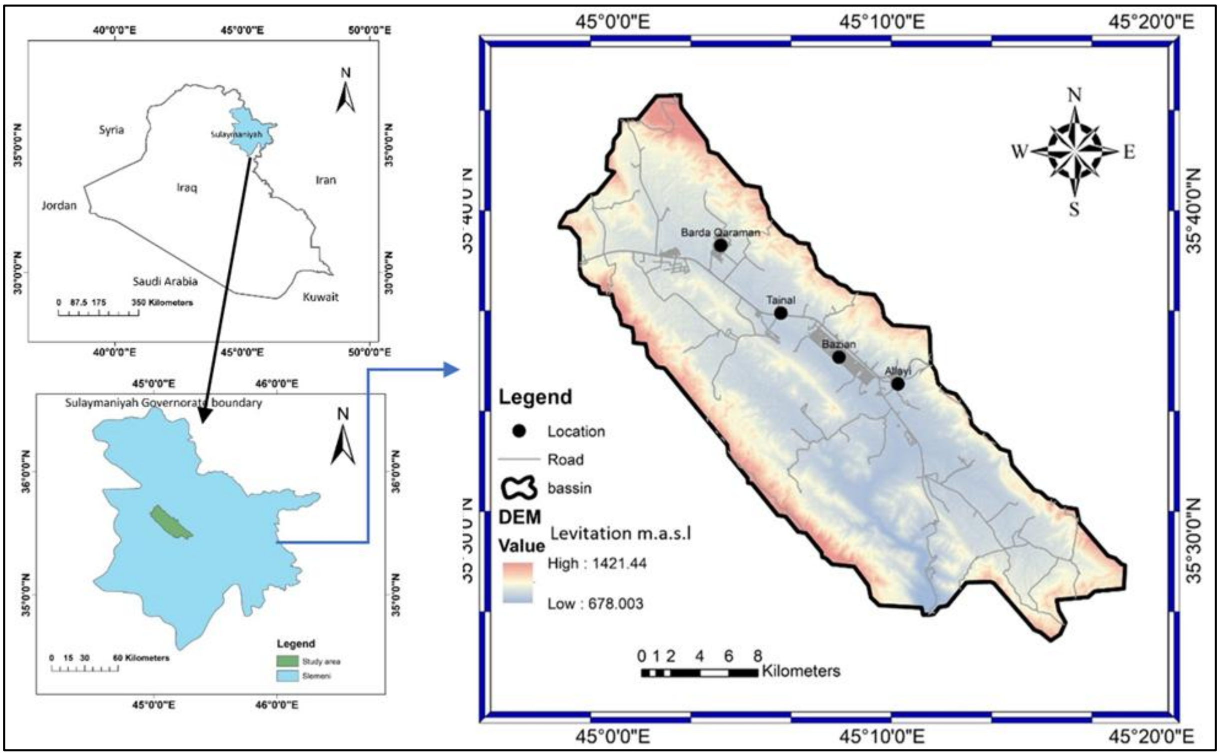

Figure 1. DEM and location map of the Bazian basin.

Geologically, the exposed formations in the region belong to the Paleocene – Early Eocene to Pleistocene sedimentary sequences (Figure 2) youngest (Aziz, 2005). The Kolosh Formation, Early Paleocene, is the oldest exposed formation in the region, whereas the Pleistocene Recent

Sediments are the youngest (Aziz, 2005).(Sissakian & Fouad, 2014) Lithologically, the Kolosh Formation primarily consists of impermeable grey to dark grey calcareous shale that alternates with siltstone and silty marlstone., The Sinjar Formation, Late Paleocene–Early Eocene, consists mainly of fissured massive yellowish limestone and sandy limestone. Gercus formation Early Middle Eocene also has a red clastic sequence of claystone and siltstone that alternates with green marl, as well as coarse-grained sandstone ranging in color from gray to reddish brown and including conglomerate beds at the base of the sandstone layers. Pilaspi Formation Middle-Late Eocene consists of a variety of limestone types, including dolomitic, chalky, and well-bedded highly fractured limestone. The recent sediments include river terraces, slope deposits, alluvial deposits, and other types of silt, mud, sand, and gravel (Ahmed & Al-Manmi, 2019; Aziz, 2005; Hamamin, 2011).

From a hydrogeological perspective, the recent sediments are recognized as the major intergranular aquifer in the basin. The Sinjar and Pilaspi aquifers are recognized as karstic-fissured aquifers, while the Kolosh and Gercus Formations are classified as aquiclude aquifers (Ali & Hamamin, 2012).

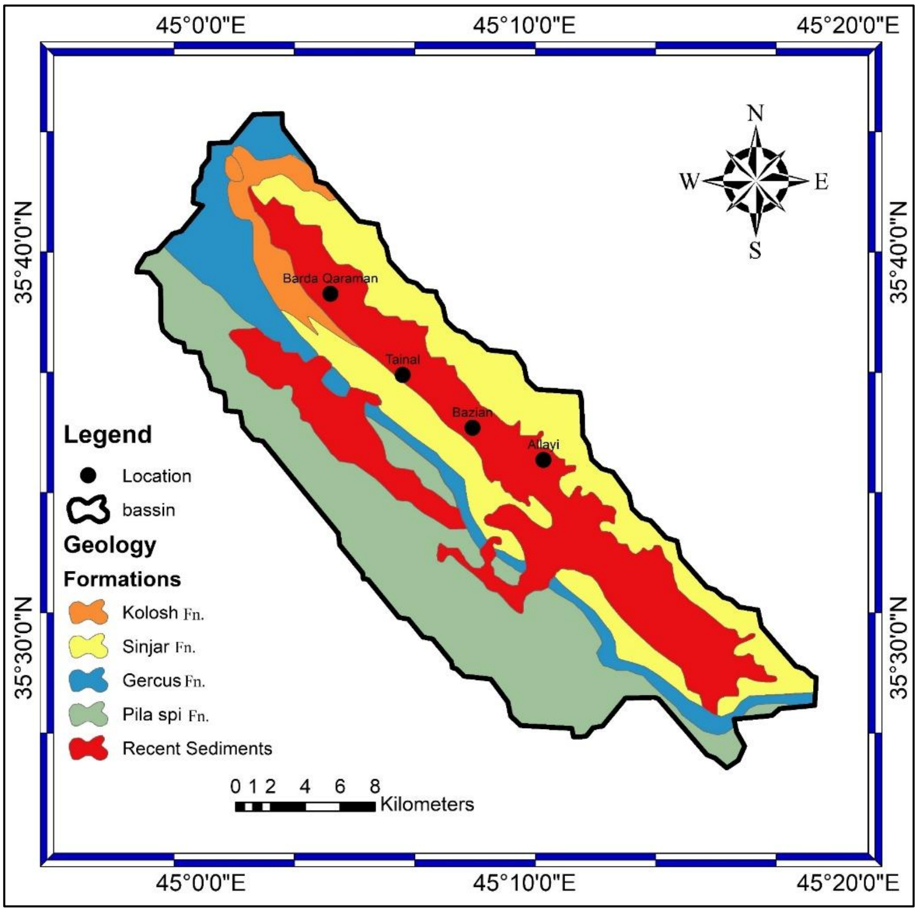

Figure 2. Geological map of the Bazian basin (Sissakian & Fouad, 2014).

3. Methodology

3.1. Data Collection and Preparation Maps

The process of integrating GIS, RS, and AHP approaches involves translating and harmonizing geographical data and weightage ranking to gather information that can be applied to decision-making (Pathmanandakumar, Thasarathan, et al., 2021; Patra et al., 2018). These techniques were employed in this article to delineate the groundwater potential zones of the Bazian basin using 7 thematic layers, such as rainfall, geology, lineament density, slope, runoff, land use/land cover, and drainage density. Table 1 lists the data sources used to generate the groundwater potential areas, and Figure 3 illustrates the complete methodology flowchart of this study.

3.2. Weight assignment using the AHP model

The most popular and widely recognized GIS-based approach for detecting zones with potential groundwater is multi-criteria decision analysis applying the analytical hierarchical process (Arulbalaji et al., 2019). This approach facilitates the combination of all thematic maps and the identification of the weight of a criterion via pairwise comparison (Saaty and L, 1980; Saaty, 1977). Expert knowledge and the literature review by many researchers are used to derive priority weights in the AHP, which is a concept of measurement by a pairwise comparison matrix (PCM) (Pathmanandakumar, Thasarathan, et al., 2021; Rajasekhar et al., 2019). The potentiality of each layer for the groundwater recharge area was considered to assigning the weights. Parameters with high values show layers with a large influence on groundwater potential, whereas those with low values show layers with a minor influence, as shown in Table 2. The relative importance of each parameter was determined using Saaty's scale (1 – 9), and the thematic layers were valued using a scale from one (equal significance) to nine (extreme significance) (Saaty, 1990). Equations (1) and (2) are then used to produce the consistency ratio (CR) and consistency index (CI), which are used to determine if these weights are consistent:

$$\mathrm{CR} = \frac{\mathrm{CI}}{\mathrm{RI}} \tag{1}$$

$$\mathrm{CI} = \lambda_{\max} - \mathrm{n}/\mathrm{n} - 1 \tag{2}$$

Where: CR stands for the consistency ratio, CI represents the consistency index, and RI is the random index, which was obtained from a table generated by Saaty in 1990. λmax is a principal eigenvalue, n denotes the number of thematic layers, and CI stands for the consistency index. The consistency ratio suggests that a suitable level would be indicated if $CR < 0.1$, whereas inconsistent judgments would be indicated if $CR > 0.1$. Additionally, a zero CR score reflects full consistency in the pairwise comparison (Gangadharan & Vinoth, 2016; Saaty, 1990). The pairwise matrix comparison in this study demonstrates excellent consistency, with the computed CR of 0.02 ($\lambda max = 7.163$, $n = 7$, $RI = 1.32$, $CI = 0.027$).

Table 1. Source information for the used data in this research.

Thematic Layers	Sources	Scale
Rainfall (Ra)	CHIRPS	0.1° 0.1°
Geology (G)	Iraqi Geological Survey	1:250000
Lineament density (Ld)	Harmonized Sentinel-2	10 m
Slope (Sp)	SRTM DEM	30 m
Runoff (Ru)	Generated by GEE from (CHIRPS, Soil texture classes) (USDA system), MODIS	0.1° 0.1°
LULC (Lu)	ESA World Cover 10m v100	10 m
Drainage density (Dd)	SRTM DEM	30 m

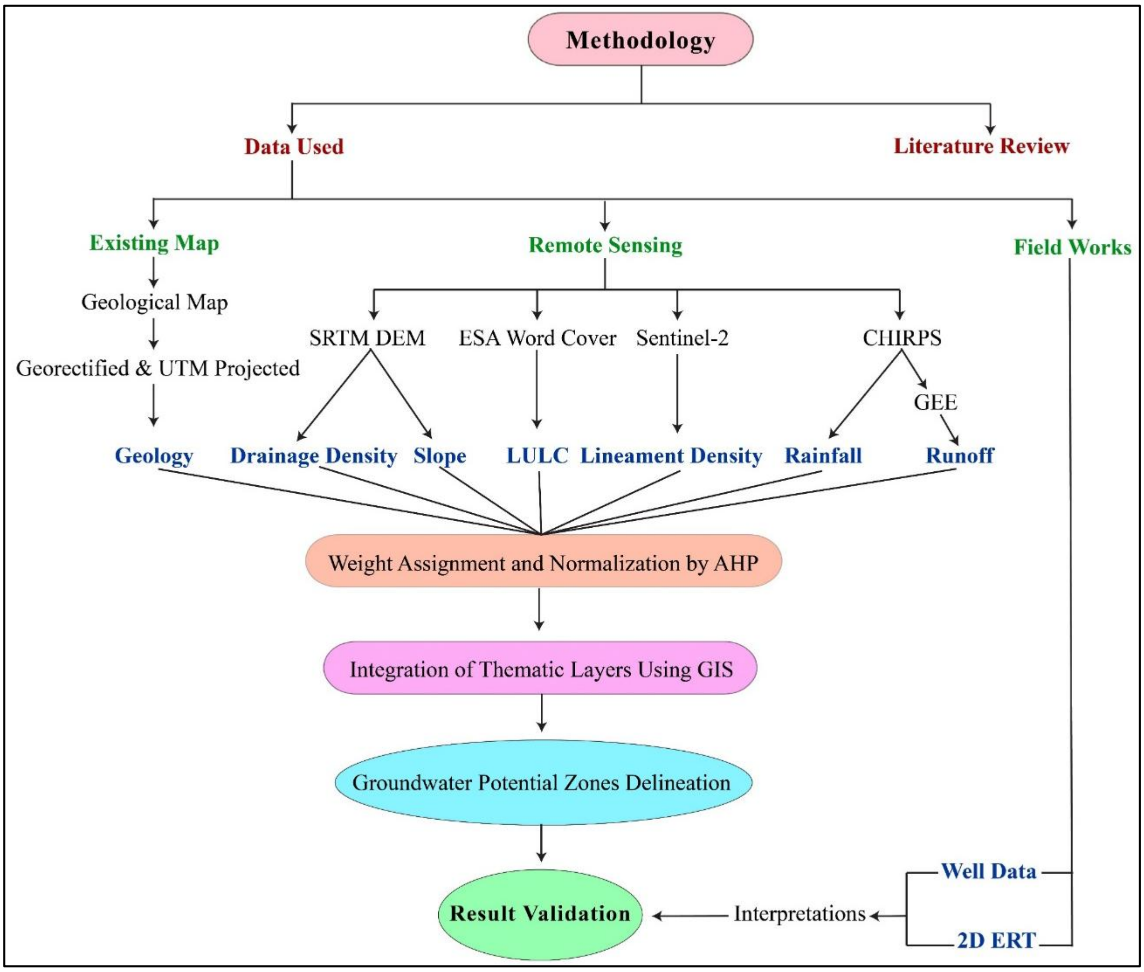

Figure 3. Methodological flowchart adapted for this study.

Table 2. Thematic layers/classes weighting for mapping of groundwater potential zones.

Thematic Layers	Features/Classes	ranks	Class weight (%)	Layer weights (%)
Rainfall (mm)	<550	5	6.1	27.9
	550 – 575	4	9.7	
	575 – 600	3	16	
	600 – 625	2	26.3	
	>625	1	41.9	
Geology	Recent sediments	1	40	24.2
	Pila spi	2	24	
	Sinjar	3	22	
	Kolosh	4	7	
	Gercus	4	7	
lineament density km/km^2	<0.75	5	6.2	16.9
	0.75 – 1	4	9.7	
	1 – 1.5	3	16	
	1.5 – 2.5	2	26.3	
	>2.5	1	41.8	
Slope(degree)	<5	1	41.9	12.8
	5 – 10	2	26.2	
	10 – 15	3	15.9	
	15 – 20	4	9.8	
	>20	5	6.2	
Runoff (mm)	<50	1	41.8	7.8
	50 – 100	2	26.2	
	100 – 150	3	15.9	
	150 – 200	4	9.9	
	>200	5	6.2	
LU/LC	Tree cover	1	22.5	6.2
	Cropland	2	20.1	
	Grassland	3	15.6	
	Shrubland	4	14.1	
	Bare/ sparse vegetation	5	12.3	
	Permanent water bodies	5	12.3	
	Built-up	6	3	
Drainage density (km/km^2)	<0.1	1	46.7	4.2
	0.1 – 0.5	2	27.8	
	0.5 – 1	3	16	
	>1		9.5	
Total				**100**

Weighted overlay analysis in ArcGIS is used to calculate the combination of the seven thematic maps with their potential weights. Furthermore, the reclassification was carried out in a GIS environment following the assignment of all normalized weights, and Equation (3) was then used to construct the groundwater potential map zones (GPMZs).

$$\mathrm{GPMZ} = \mathrm{Ra_{lw}Ra_{cw}} + \mathrm{G_{lw}G_{cw}} + \mathrm{Ld_{lw}Ld_{cw}} + \mathrm{Sp_{lw}Sp_{cw}} + \mathrm{Ru_{lw}Ru_{cw}} + \mathrm{Lu_{lw}Lu_{cw}} + \mathrm{Dd_{lw}Dd_{cw}}) \quad (3)$$

Where GPMZ is groundwater potential map zones, Ra is for rainfall, G is for Geology, Ld is for lineament density, Sp is for the slope, Ru is for runoff, Lu is for land use/land cover, Dd is for drainage density, lw is a layer normalized weight, and cw is an individual normalized class weight. The research region is divided into five zones with varying groundwater potential: low, very low, moderate, high, and very high. This is done by allocating weights to each of these thematic layers.

3.3. Validation Methodology

Electrical resistivity tomography is an effective geophysical technique used to detect the subsurface resistivity distribution ((Rajendran et al., 2020). It is a non-destructive technique for imaging the subsurface resistivity variations of both lateral and vertical changes, presenting a variety of lithological and hydro-geological structural underlays. El Bastawesy et al. (2019). Since resistivity varies in both horizontal and vertical directions across each survey line, a 2D model of the subsurface from ERT provides more precise results. Recently, the ERT technique has become one of the best approaches for the validation of the GWPZ study, as illustrated in Figure 3. The 2D subsurface resistivity was obtained by using the SYSCAL R1 PLUS instrument, which is a multi-electrode resistivity meter system. The data was collected along three ERT profiles with a length of 710 m, with an electrode spacing of 10 m, and a Wenner–Schulmberger array was applied for data acquisition. The RES2DINV software was applied for processing and interpreting field apparent resistivity data. Additionally, data from the pumping of 40 water wells were collected and utilized to validate the groundwater potential zones, as illustrated in Figure 3.

4. Results

4.1. Rainfall

Rainfall is one of the most important parameters that influence the amount of water that precipitates in the basin area (Razandi et al., 2015). Due to the lack of metrological data for the nearby study area, a spatial rainfall map is created based on data obtained from Climate Hazards Center InfraRed Precipitation with Station data (CHIRPS) from 2000 to 2023 (Funk et al., 2015). The pair-wise comparison result shows that the first important groundwater conditioning factor is rainfall, as obtained a normalized weight of 27.9%. The annual precipitation of the area ranges from 546 to 651 mm, and the rainfall layer classifies into five categories based on potentiality from very low to very high (less than 550, 550.1 – 75, 575.1 – 600, 600.1 – 625 and more than 625 mm), and each class has percentage weight of (6%, 10%, 16%, 26%, 42%) respectively with area coverage (1%, 25.2%, 44.5%, 19.8%, 9.5%) which show in Figure 4A.

4.2. Geology

Geological formations play a crucial role in the accumulation of groundwater and in assessing the groundwater potential of a basin. The primary porosity, permeability, lithology, and thickness of rocks significantly impact this. It’s also important to consider whether the rainfall conditions contribute to increased groundwater storage and yield (Pathmanandakumar, Nadarajapillai, et al., 2021). In the Bazian basin, the main lithological units are shown in the table. Geology is the second most significant factor with a normalized weight of 24.2% used to determine the GWPZs of the area Figure 4B. The study area was classified into five categories depending on their lithological properties and importance of groundwater, sorted from very low impact to very high impact classes (Gercus 7%, Kolosh 7%, Sinjar 22%, Pila spi 24%, and

Recent sediments 40%), with area distribution coverage (11.4%, 4%, 24.1, 30.6% and 29.9%) respectively.

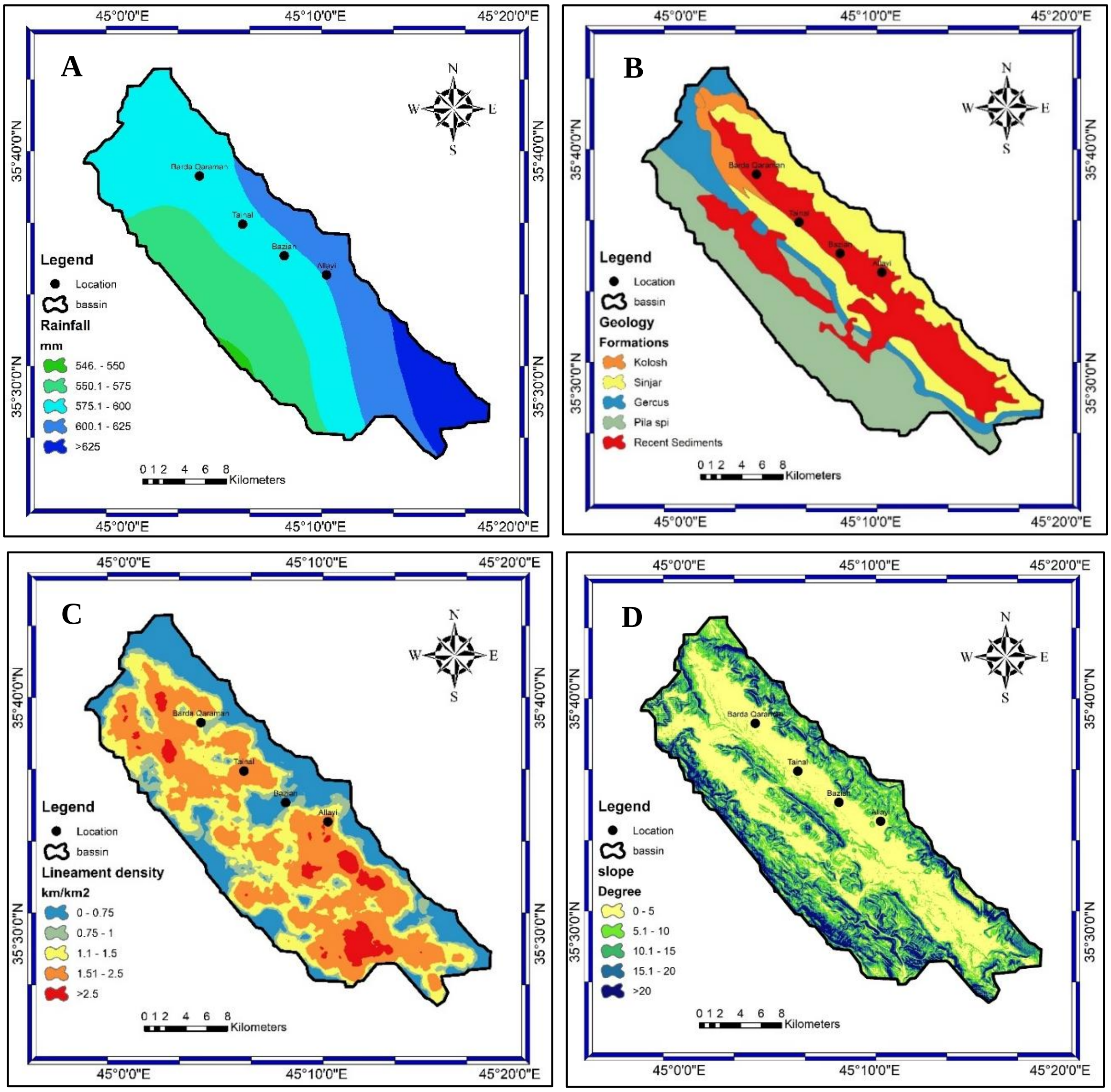

Figure 4. Thematic layers of the study area: A) Rainfall, B) geology, C) lineament density, and D) slope.

4.3. Lineament Density

Lineaments are indicators of fractures and faults in subsurface areas (Ahirwar et al., 2020). The lineaments increase secondary porosity and permeability and therefore improve groundwater existence and movement (Lemacha, 2008). A lineament distribution for the area extracted from Harmonized Sentinel-2 images, with cell size (10 m) resolution and using PCI Geomatica (2016) software. The pair-wise comparison results of Lineaments become third order with a weight of 16.9%. The lineament density of the area calculated by GIS with the unit (km/km^2) ranged from 0.25 to 4 km/km^2 categories from very high to very low are (0.25, 0.26 – 1, 1.01 –

1.5, 1.51 – 25, >2) with a weight percentage of (6.2%, 9.7%, 16%, 26.3%, and 41.8%), respectively in Figure 4C.

4.4. slope

The slope map of the basin was generated from the STRM DEM with a 30m resolution. The slope's weight percentage is 12.8%, ranking it as the fourth criterion. The study area is divided into five classes based on slope variation. Areas with a slope of 0 – 5° are considered "very good" due to the flat terrain and reduced runoff. The central part of the study area, with slopes of (0 – 5° and 5.1 – 10°), is deemed (very good to good) and is favorable for groundwater recharge. The region between the plain and mountain, with slopes of (10.1 – 15° and 15.1 – 20°), is classified as (moderate to low) for infiltration. Areas with slopes greater than 20° are considered (poor) due to steep slopes causing higher runoff. The slope map of the study area is shown in Figure 4D.

4.5. Runoff

The runoff map was created using Google Earth Engine (GEE), a robust cloud-based platform for large-scale environmental data analysis. To generate the runoff map, necessary datasets such as DEM for terrain analysis, precipitation data for rainfall input, and land cover data for surface characteristics were imported. The SCS Curve Number method was used to estimate runoff, with GEE automatically calculating the curve number and applying the runoff equation with initial abstraction. The runoff map of the basin was then exported as a raster file from GEE. The weight percentage of runoff is 7.8%. The area's rainfall ranges from 546 to 651 mm, with 42 – 284 mm becoming direct runoff shown in Figure 5A. As runoff increases, groundwater potential decreases. The area is classified into five categories based on potentiality, ranging from high to low: less than 50, 50 – 100, 101 – 150, 151 – 200, and greater than 200 mm.

4.6. Land Use/Land Cover

Land use and land cover (LULC) significantly influence groundwater dynamics by either reducing runoff and enhancing infiltration or by increasing surface runoff and hindering infiltration. The LULC map for the study area, derived from the European Space Agency's (ESA) World Cover 10 m 2020 product, offers a global land cover map at a 10 m resolution using Sentinel-1 and Sentinel-2 data. This map categorizes the basin area into seven classes. The pair-wise comparison weight percentage is 6.2%, with the categories ranked from highest to lowest as follows: Tree cover (22.5%), Cropland (20.1%), Grassland (15.6%), Shrubland (14.1%), Bare/sparse vegetation (12.3%), Permanent water bodies (12.3%), and Built-up areas (3%), shown in Figure 5 B.

4.7. Drainage Density

Drainage density indirectly affects the suitability of groundwater formation due to its relationship with infiltration capacity and permeability. Higher drainage density reduces water infiltration into groundwater zones, resulting in increased runoff and vice versa. Drainage density refers to the closeness of stream channels within an area and is calculated as the ratio of the total length of streams to the total area (Tanny et al., 2008). Drainage density was determined using STRM DEM 30m data with the spatial analyst extension in ArcMap, measured in units of km/km² Figure 5C. The overall weight percentage is 4.2%, and the area is classified into four categories based on potential, from low to high: more than 1 (9%), 0.51 – 1 (16%), 0.1 – 0.5 (27.8%), and less than 0.1 (46.7%).

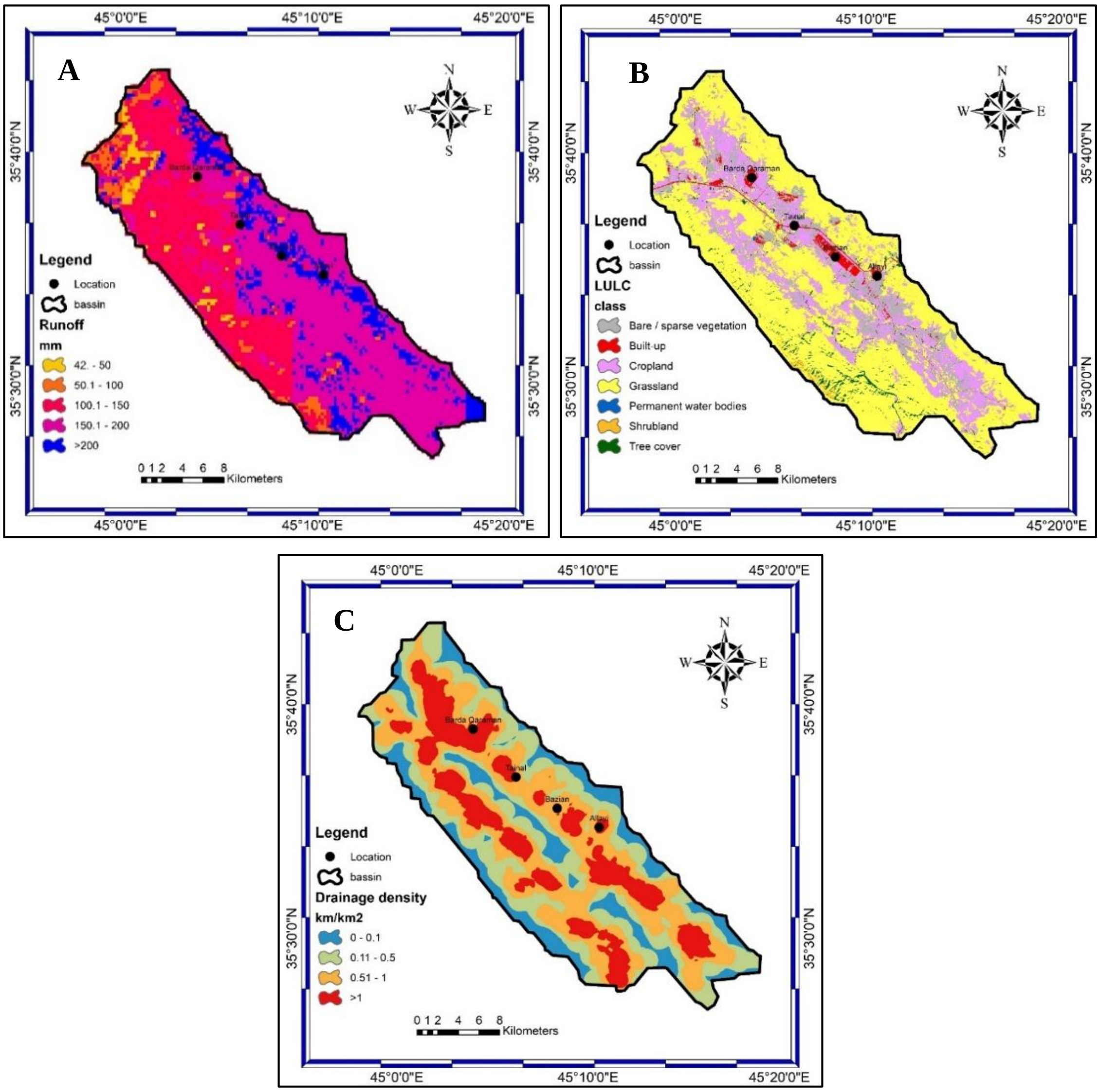

Figure 5. A) Runoff, B) LU/LC, and C) drainage density.

5. Discussion

5.1. GWPZs Delineation

Groundwater potential zones are identified through the integration of Geographic Information Systems (GIS), Remote Sensing (RS), and the Analytical Hierarchy Process (AHP). The potential map for the study area is produced by assigning weights to seven thematic maps and their respective attributes. These datasets are then integrated into the GIS framework using Equation (3). All reclassified input layers were merged in GIS using raster calculation techniques to create the final groundwater potential map, utilizing a weighted linear combination approach (Malczewski, 1999). Groundwater potential zones (GWPZs) are classified into five categories: very low, low, moderate, high, and very high (Figure 6). The spatial distribution indicates that the very low and low zones are concentrated along the northern and southern boundaries of the basin, covering 4.4% and 8.9% of the study area, respectively. The moderate zone is scattered in various locations between the low and high zones, accounting for 34.3% of the area. The high and very high zones cover 32.7% and 19.7% of the study area, respectively, and are primarily located in the center of the basin where recent sediments are exposed, making these areas suitable for groundwater drilling and exploitation Table 3.

Table 3. GWPZs, coverage area, and percentages.

Class of GWPZs	Area of Coverage (km^2)	Area (%)
Very low	15.7	4.4
Low	32.1	8.9
Moderate	124.2	34.3
High	118.5	32.7
Very high	71.4	19.7

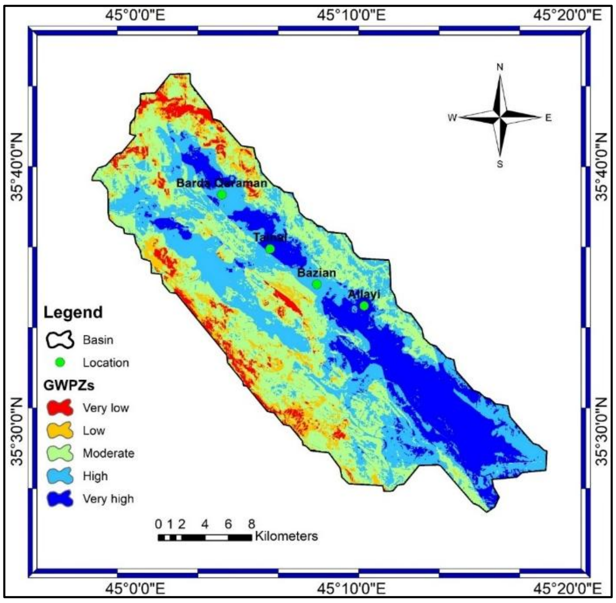

Figure 6. GWPZs of the Bazin basin.

5.2. Groundwater Potential Zone Validation

Two methods are used for validation first three ERT profiles were obtained for validation of GWPZs of the Bazian basin, as shown in Figure 7. Since 2D ERT is a time-consuming and costly method, it was conducted in the moderate class very high-potential zone. Furthermore, the presence of high-ridge mountains, urban areas, and fenced agricultural lands made conducting a geophysical survey difficult in this study.

The first profile is in the medium GWPZs and has a resistivity value range between 5 – 25 Ωm, Figure 8. Generally, this profile is composed of three zones depending on the resistivity value distribution. The resistivity value of the first zone ranges between 5 – 10 Ωm, composed of shale, and starts from a depth of 53 m to the maximum depth of the investigation. Since this layer is impermeable, it has very low GWPZs. The second zone has a resistivity value range between 10 – 16 Ωm, composed of silt, sand, and a little clay from a recent deposit. The thickness of this zone ranges from 0 to 53 m under electrodes 20 to 72. This zone represents medium GWPZs due to the presence of clay. The third zone has a resistivity value range between 16 – 25 Ωm, composed of gravel and sand from a recent deposit. It has a thickness ranging from 0 to 53 m under electrodes 1 to 20. This zone represents the very high GWPZs due to the absence of clay. The second and third profiles are in very high GWPZs, as shown in Figure 7. They are composed of two main zones, as shown in Figure 8. The resistivity value of the first zone ranges between 4 – 9 Ωm, composed of shale of the Kolosh formation. Also, the second zone resistivity value ranges between 9 – 30 Ωm, composed of a mixture of sand, gravel, silt, and some clay of the recent deposit. The thickness of this zone for the second and third profiles ranges from 0 to 50 m and 0 to 100 m, respectively. As a result, this zone has very high GWPZs due to its low clay content and good aquifer thickness. The second method involves measuring the extraction rate of water wells in the basin area, with data collected from 40 water wells. These rates are categorized into three groups: less than 2 Liters/sec (low), 2.1 – 5 Liters/sec (moderate), and more than 5 Liters/sec (high), 65% of high extraction rate wells are in very high potential zones, while 35% are in high potential zones 62% of moderate extraction rate wells are in high potential zones, with the remaining percentage in very high potential zones. 40% of low-extraction-rate wells are in low and very low potential zones. Statistical and spatial distribution of wells shows that GWPZs and extraction rates of wells coincide with each other and prov**e** to be an effective validation technique.

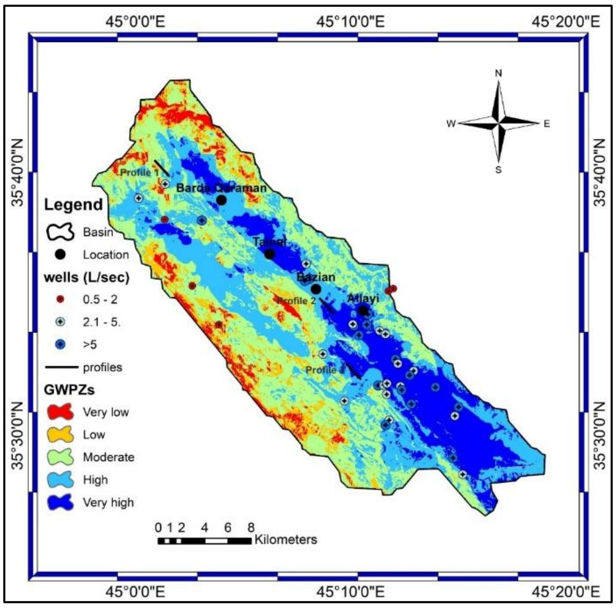

Figure 7. GWPZs with the location of validation ERT profiles and wells.

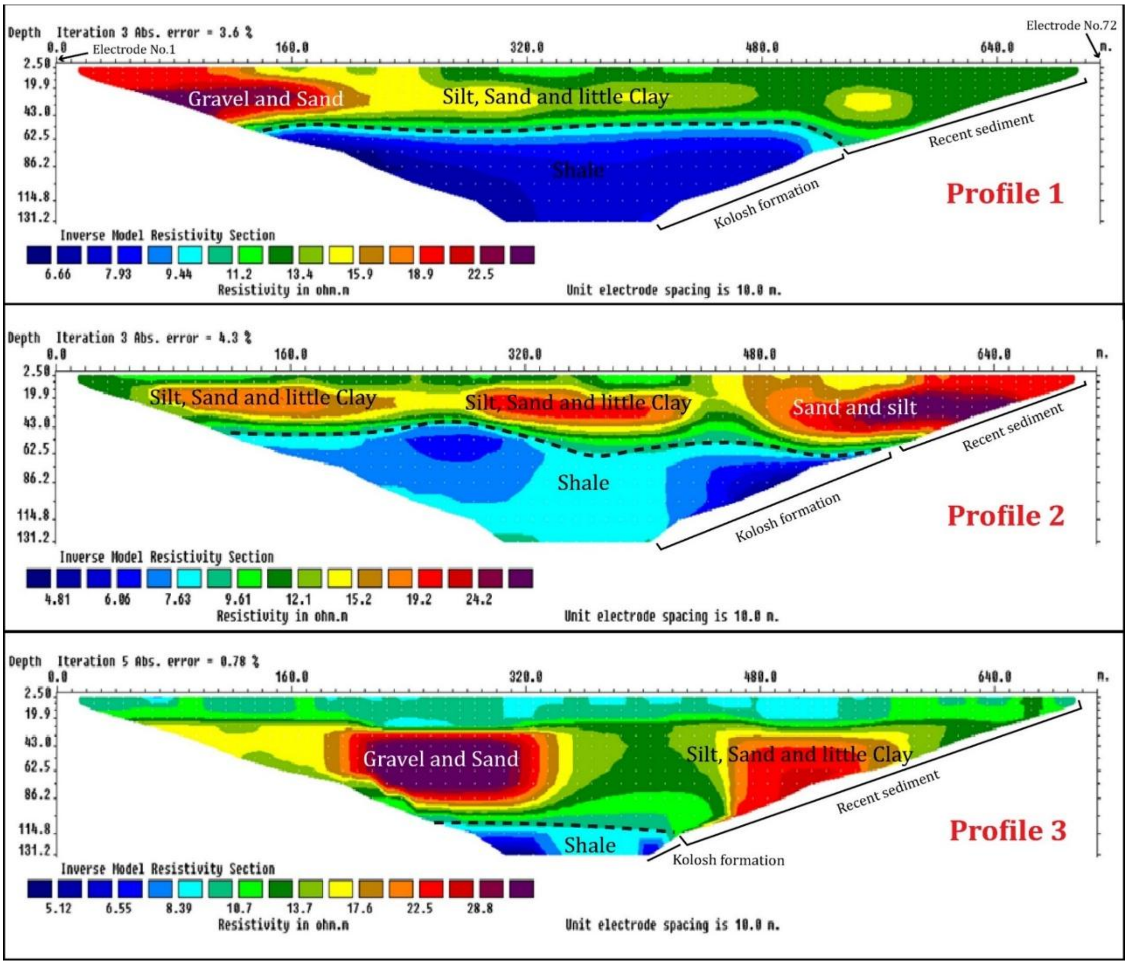

Figure 8. Validated 2D ERT profiles.

6. Conclusions

The study successfully identifies groundwater potential zones (GWPZs) using GIS, Remote Sensing (RS), Electrical Resistivity Tomography (ERT), and the Analytical Hierarchy Process (AHP). By integrating seven thematic maps into a GIS framework, a final groundwater potential map is produced. The GWPZs are categorized into five levels: very low, low, moderate, high, and very high. ERT and water wells extraction rate are a good combination for validation of the groundwater potential zones (GWPZs) in the Bazian basin. The spatial distribution reveals that the high and very high zones, which are ideal for groundwater drilling, are mainly located in the center of the basin with high pumping rates. Given the limitations of this study, the analytical hierarchy process (AHP) may lack realism due to its common reliance on surface-level factors like topography, slope, exposed lithology, and land use/land cover. These factors do not fully capture the subsurface characteristics of the aquifer. To address this, future assessments should consider aquifer type, hydraulic properties, saturated thickness, groundwater levels, and groundwater quality.

References

Ahirwar, S., Malik, M. S., Ahirwar, R., & Shukla, J. P. (2020). Application of remote sensing and GIS for groundwater recharge potential zone mapping in Upper Betwa Watershed. *Journal of the Geological Society of India*, *95*, 308–314.

Ahmed, T. H., & Al-Manmi, D. A. M. (2019). Delineation of groundwater productivity zones with the integration of GIS and remote sensing methods, Bazian Basin, Sulaymaniyah, Kurdistan Region, Iraq. *Journal of Basrah Researches (Sciences)*, *2*(2).

Al-Abadi, A. M., Al-Temmeme, A. A., & Al-Ghanimy, M. A. (2016). A GIS-based combining of frequency ratio and index of entropy approaches for mapping groundwater availability zones at Badra–Al Al-Gharbi–Teeb areas, Iraq. *Sustainable Water Resources Management*, *2*, 265–283.

Al-Garni, M. A. (2009). Geophysical investigations for groundwater in a complex subsurface terrain, Wadi Fatima, KSA: A case history. *Jordan Journal of Civil Engineering*, *3*(2), 118–136.

Ali, S. S., & Hamamin, D. F. (2012). Groundwater Vulnerability Map of Basara Basin, Sulaimani Governorate, Iraqi Kurdistan Region. *Iraqi Journal of Science*, *53*(3), 579–594.

Al-Manmi, D. A. M., & Rauf, L. F. (2016). Groundwater potential mapping using remote sensing and GIS-based, in Halabja City, Kurdistan, Iraq. *Arabian Journal of Geosciences*, *9*(5), 1–13.

Andualem, T. G., & Demeke, G. G. (2019). Groundwater potential assessment using GIS and remote sensing: A case study of Guna tana landscape, upper blue Nile Basin, Ethiopia. *Journal of Hydrology: Regional Studies*, *24*, 100610.

Arulbalaji, P., Padmalal, D., & Sreelash, K. (2019). GIS and AHP techniques based delineation of groundwater potential zones: a case study from southern Western Ghats, India. *Scientific Reports*, *9*(1), 1–17.

Ayazi, M. H., Pirasteh, S., Arvin, A. K. P., Pradhan, B., Nikouravan, B., & Mansor, S. (2010). Disasters and risk reduction in groundwater: Zagros Mountain Southwest Iran using geoinformatics techniques. *Disaster Adv*, *3*(1), 51–57.

Aziz, B. Q. (2005). Two dimension resistivity imaging tomography for hydrogeological study in Bazian basin, west Sulaimani city, NE-Iraq. *Unpublished Ph. D. Thesis, University of Sulaimani, Sulaymaniyah, Iraq*.

Barzinji, K. T. (2003). *Hydrogic Studies for Goizha Dabashan and Other Watersheds in Sulimani Governorate*. M. Sc. thesis submitted to the College of Agriculture, University of Sulaimania.

Chenini, I., Mammou, A. Ben, & El May, M. (2010). Groundwater recharge zone mapping using GIS-based multi-criteria analysis: a case study in Central Tunisia (Maknassy Basin). *Water Resources Management*, *24*(5), 921–939.

Chowdary, V. M., Chakraborthy, D., Jeyaram, A., Murthy, Y. V. N., Sharma, J. R., & Dadhwal, V. K. (2013). Multi-criteria decision making approach for watershed prioritization using analytic hierarchy process technique and GIS. *Water Resources Management*, *27*(10), 3555–3571.

Chowdhury, A., Jha, M. K., & Chowdary, V. M. (2010). Delineation of groundwater recharge zones and identification of artificial recharge sites in West Medinipur district, West Bengal, using RS, GIS and MCDM techniques. *Environmental Earth Sciences*, *59*(6), 1209–1222.

Das, B., & Pal, S. C. (2019). Combination of GIS and fuzzy-AHP for delineating groundwater recharge potential zones in the critical Goghat-II block of West Bengal, India. *HydroResearch*, *2*, 21–30.

El Bastawesy, M., Attwa, M., Hafeez, T. H. A., & Gad, A. (2019). Flash floods and groundwater evaluation for the non-gauged dryland catchment using remote sensing, GIS and DC resistivity data: A case study from the Eastern Desert of Egypt. *Journal of African Earth Sciences*, *152*, 245–255.

Fitts, C. R. (2002). *Groundwater science*. Elsevier.

Funk, C., Peterson, P., Landsfeld, M., Pedreros, D., Verdin, J., Shukla, S., Husak, G., Rowland, J., Harrison, L., & Hoell, A. (2015). The climate hazards infrared precipitation with stations—a new environmental record for monitoring extremes. *Scientific Data*, *2*(1), 1–21.

Gangadharan, R., & Vinoth, S. (2016). Assessment of groundwater vulnerability mapping using AHP method in coastal watershed of shrimp farming area. *Arabian Journal of Geosciences*, *2*(9), 1–14.

Hajkowicz, S., & Higgins, A. (2008). A comparison of multiple criteria analysis techniques for water resource management. *European Journal of Operational Research*, *184*(1), 255–265.

Hamamin. (2011). *HYDROGEOLOGICAL ASSESSMENT AND GROUNDWATER VULNERABILITY MAP OF BASARA BASIN, SULAIMANI GOVERNORATE, IRAQI KURDISTAN REGION*. Sulaimani.

Islami, N., Taib, S. H., Yusoff, I., & Ghani, A. A. (2018). Integrated geoelectrical resistivity and hydrogeochemical methods for delineating and mapping heavy metal zone in aquifer system. *Environmental Earth Sciences*, *77*(10), 1–18.

Jha, M. K., Chowdhury, A., Chowdary, V. M., & Peiffer, S. (2007). Groundwater management and development by integrated remote sensing and geographic information systems: prospects and constraints. *Water Resources Management*, *21*(2), 427–467.

Kaliraj, S., Chandrasekar, N., & Magesh, N. S. (2014). Identification of potential groundwater recharge zones in Vaigai upper basin, Tamil Nadu, using GIS-based analytical hierarchical process (AHP) technique. *Arabian Journal of Geosciences*, *7*(4), 1385–1401.

Karim, H. A., & Al-Manmi, D. A. (2019). Integrating GIS-based and geophysical techniques for groundwater potential assessment in Halabja Said Sadiq sub-basin, Kurdistan, NE Iraq. *Tikrit Journal of Pure Science*, *24*(6), 81–92.

Kowalsky, M. B., Gasperikova, E., Finsterle, S., Watson, D., Baker, G., & Hubbard, S. S. (2011). Coupled modeling of hydrogeochemical and electrical resistivity data for exploring the impact of recharge on subsurface contamination. *Water Resources Research*, *47*(2).

Kumari, A., Kumar, D., & Warwade, P. (2021). Application of multi-criteria decision making (MCDM) and electrical resistivity tomography (ERT) techniques for identification of groundwater recharge zone (s) in granitic hard rock aquifer. *Journal of Earth System Science*, *130*(2), 1–17.

Lemacha, G. (2008). Groundwater potential for upper Tumet catchment, Merge and Komosha woredas, Benishangul-Gumuz region. *Guide for GIS Developers, WaterAid Ethiopia and Ripple Www. Rippleethiopia. Org*.

Madani, A., & Niyazi, B. (2015). Groundwater potential mapping using remote sensing techniques and weights of evidence GIS model: a case study from Wadi Yalamlam basin, Makkah Province, Western Saudi Arabia. *Environmental Earth Sciences*, *74*(6), 5129–5142.

Malczewski, J. (1999). *GIS and multicriteria decision analysis*.

Naghibi, S. A., Pourghasemi, H. R., & Abbaspour, K. (2018). A comparison between ten advanced and soft computing models for groundwater qanat potential assessment in Iran using R and GIS. *Theoretical and Applied Climatology*, *131*(3), 967–984.

Naghibi, S. A., Pourghasemi, H. R., & Dixon, B. (2016). GIS-based groundwater potential mapping using boosted regression tree, classification and regression tree, and random forest machine learning models in Iran. *Environmental Monitoring and Assessment*, *188*(1), 1–27.

Nampak, H., Pradhan, B., & Abd Manap, M. (2014). Application of GIS based data driven evidential belief function model to predict groundwater potential zonation. *Journal of Hydrology*, *513*, 283–300.

Oh, H.-J., Kim, Y.-S., Choi, J.-K., Park, E., & Lee, S. (2011). GIS mapping of regional probabilistic groundwater potential in the area of Pohang City, Korea. *Journal of Hydrology*, *399*(3–4), 158–172.

Ozdemir, A. (2011). GIS-based groundwater spring potential mapping in the Sultan Mountains (Konya, Turkey) using frequency ratio, weights of evidence and logistic regression methods and their comparison. *Journal of Hydrology*, *411*(3–4), 290–308.

Pathmanandakumar, V., Nadarajapillai, T., & Manjula, R. (2021). An Approach to Delineate Potential Groundwater Zones in Kilinochchi District. *Using GIS Techniques, Sri Lanka*.

Pathmanandakumar, V., Thasarathan, N., & Ranagalage, M. (2021). An Approach to Delineate Potential Groundwater Zones in Kilinochchi District, Sri Lanka, Using GIS Techniques. *ISPRS International Journal of Geo-Information*, *10*(11), 730.

Patra, S., Mishra, P., & Mahapatra, S. C. (2018). Delineation of groundwater potential zone for sustainable development: A case study from Ganga Alluvial Plain covering Hooghly district of India using remote sensing, geographic information system and analytic hierarchy process. *Journal of Cleaner Production*, *172*, 2485–2502.

Rahmati, O., Nazari Samani, A., Mahdavi, M., Pourghasemi, H. R., & Zeinivand, H. (2015). Groundwater potential mapping at Kurdistan region of Iran using analytic hierarchy process and GIS. *Arabian Journal of Geosciences*, *8*(9), 7059–7071.

Rajasekhar, M., Raju, G. S., Sreenivasulu, Y., & Raju, R. S. (2019). Delineation of groundwater potential zones in semi-arid region of Jilledubanderu river basin, Anantapur District, Andhra Pradesh, India using fuzzy logic, AHP and integrated fuzzy-AHP approaches. *HydroResearch*, *2*, 97–108.

Rajendran, G., Mohammed, M., Shivakumar, S., Merera, W., & Taddese, K. (2020). Geospatial techniques amalgamated with two-dimensional electrical resistivity imaging for delineation of groundwater potential zones in West Guji Zone, Ethiopia. *Groundwater for Sustainable Development*, *11*, 100407.

Razandi, Y., Pourghasemi, H. R., Neisani, N. S., & Rahmati, O. (2015). Application of analytical hierarchy process, frequency ratio, and certainty factor models for groundwater potential mapping using GIS. *Earth Science Informatics*, *8*, 867–883.

Saaty, & L, T. (1980). *The analytical hierarchy process: Planning, priority setting, resources allocation*. McGraw-Hill, New York.

Saaty, T. L. (1977). A scaling method for priorities in hierarchical structures. *Journal of Mathematical Psychology*, *15*(3), 234–281.

Saaty, T. L. (1990). *Decision making for leaders: the analytic hierarchy process for decisions in a complex world*. RWS publications.

Sangawi, A., Al-Manmi, D. A. M., & Aziz, B. Q. (2023). Integrated GIS, remote sensing, and electrical resistivity tomography methods for the delineation of groundwater potential zones in Sangaw Sub-Basin, Sulaymaniyah, KRG-Iraq. *Water*, *15*(6), 1055.

Singh, K. K. K., Bharti, A. K., Pal, S. K., Prakash, A., Saurabh, Kumar, R., & Singh, P. K. (2019). Delineation of fracture zone for groundwater using combined inversion technique. *Environmental Earth Sciences*, *78*, 1–12.

Sissakian, V. K., & Fouad, S. F. (2014). Geological map of Sulaimaniyah Quadrangle, scale 1: 250000. *Iraq Geological Survey Publications, Baghdad, Iraq*.

Sonkamble, S., Satishkumar, V., Amarender, B., & Sethurama, S. (2014). Combined ground-penetrating radar (GPR) and electrical resistivity applications exploring groundwater potential zones in granitic terrain. *Arabian Journal of Geosciences*, *7*(8), 3109–3117.

Tanny, J., Cohen, S., Assouline, S., Lange, F., Grava, A., Berger, D., Teltch, B., & Parlange, M. B. (2008). Evaporation from a small water reservoir: Direct measurements and estimates. *Journal of Hydrology*, *351*(1–2), 218–229.

Venkateswaran, S., Prabhu, M. V., & Karuppannan, S. (2014). Delineation of groundwater potential zones using geophysical and GIS techniques in the Sarabanga Sub Basin, Cauvery River, Tamil Nadu, India. *Int J Curr Res Acad Rev*, *2*(1), 58–75.

About the author

Hawber Ata Karim is an assistant lecturer at the Department of Earth Science and Petroleum, College of Science, University of Sulaimani. He was awarded his B.Sc. in geology in 2010, and an M.Sc. in Hydrogeology in 2020. Hawber worked on different hydrological and geophysical projects from 2012 – 2024. As well as a member of Kurdistan Geological Society 2010-till now. Supervisor of hydrological and Picarro isotope analyzer lab at the Earth Science and Petroleum Department 2020 – 2024. He supervised many undergraduate student research in his area of expertise.

e-mail: hawber.karim@univsul.edu.iq

Zana Mahmood Mohammed Faraj Rughzai is an assistant lecturer at the Department of Earth Science and Petroleum, College of Science, University of Sulaimani. He was awarded his B.Sc. in geology in 2010, and an M.Sc. in Geophysics in 2022. Zana worked on different geophysical projects from 2012 – 2024. As well as a member of the Kurdistan Geological Society 2010-till now.

e-mail: zana.faraj@univsul.edu.iq

Dr. Azad Taher Kareem (Azad Sangawi) is an assistant professor at the University of Sulaimani. He graduated from the University of Sulaimani with a B.Sc. degree in geology and was awarded an MSc degree in 2012 from Newcastle University, UK, in the field of applied hydrogeology. He also was awarded a PhD degree in 2023 at the University of Sulaimani in the field of groundwater management. He has 12 years of experience working in the field of hydrogeology, teaching courses like hydrology, hydrogeology, and groundwater modeling and researching. He published several articles in international and local journals and supervised many BSc students in Iraq. He is a member of the Kurdistan Geologists Society.

e-mail: azad.kareem@univsul.edu.iq